# **ORGANOMETALLICS**

pubs.acs.org/Organometallics Article

# Late 3*d*-Transition Metal Complexes Bearing a *Bis*-Phosphine Borane Ligand, PhB(CH<sub>2</sub>P<sup>t</sup>Bu<sub>2</sub>)<sub>2</sub>

Rex C. Handford, Lingfei Zhong, and T. Don Tilley\*



Cite This: Organometallics 2022, 41, 2631–2637



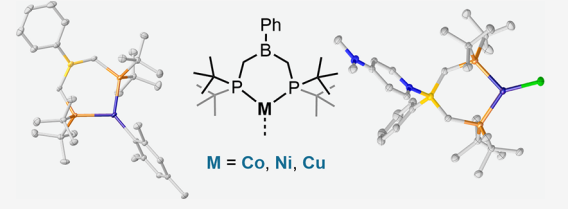
**ACCESS** I

III Metrics & More

Article Recommendations

Supporting Information

**ABSTRACT:** The coordination chemistry of a bidentate ambiphilic ligand, PhB(CH<sub>2</sub>P<sup>f</sup>Bu<sub>2</sub>)<sub>2</sub> ([BP<sub>2</sub><sup>fBu</sup>]), is established for a series of Co, Ni, and Cu compounds. The chloride starting materials [BP<sub>2</sub><sup>fBu</sup>]MCl<sub>2</sub> [M = Co ( $\mathbf{1}_{Co}$ ), Ni ( $\mathbf{1}_{Ni}$ )] and [BP<sub>2</sub><sup>fBu</sup>]CuCl ( $\mathbf{2}_{Cu}$ ) are readily accessed in high yields by the treatment of the corresponding metal chloride salts with [BP<sub>2</sub><sup>fBu</sup>] in THF solution. The reduction of  $\mathbf{1}_{Ni}$  to [BP<sub>2</sub><sup>fBu</sup>]NiCl ( $\mathbf{2}_{Ni}$ ) was affected by treatment with KC<sub>8</sub>. In contrast, the corresponding Co<sup>I</sup> species was not isolable under similar reaction conditions. However, monovalent mesityl complexes of the



form  $[BP_2^{fBu}]M(Mes)$   $[M = Co\ (3_{Co}), Ni\ (3_{Ni}), Cu\ (3_{Cu})]$  were prepared by the treatment of  $1_{Co}$  with one equiv of  $Mes_2Mg(THF)_2$  or by the reaction of  $2_M$  (M = Ni, Cu) with 0.5 equiv of  $Mes_2Mg(THF)_2$ . Modification of the borane moiety in  $2_{Ni}$  was explored by the treatment of this complex with 4-dimethylaminopyridine (DMAP) to produce  $[PhB(DMAP)(CH_2P^tBu_2)_2]NiCl\ (4)$ , which displays distinct features in its UV-visible spectrum compared to  $2_{Ni}$ . The solid-state molecular structures of most complexes have been determined by single-crystal X-ray diffraction analysis.

### INTRODUCTION

Transition-metal complexes bearing ambiphilic ligands (with both donor and acceptor centers) are of interest as such species provide new pathways for substrate activations involving the metal and acceptor sites. 1-4 Prominent examples are bis- and tris-phosphinoborane ligands which allow close contact of the metal and boron centers and formation of M  $\rightarrow$ B (Z-type) interactions.  $^{1,4-8}$  The latter bonding feature is particularly common in complexes of low-valent metal centers, where additional electron density from the metal center can be shared with boron.<sup>8</sup> For instance, close M-B contacts are observed in  $[PhB(\textit{o-}C_6H_4P^iPr_2)_2]Co(N_2)^9$  and  $[MesB(\textit{o-}C_6H_4PPh_2)_2]Ni$  (Mes = mesityl).  $^{10}$  The M–B linkages in these species cooperatively participate in bond activations by accepting fragments of incoming substrates. 11-15 For example, the reaction of these Co or Ni species with silanes results in the formation of M-Si linkages and a M( $\mu_2$ -H)B moiety (Figure 1a).<sup>9,10</sup>

In this laboratory, bis-phosphinoborane complexes have been encountered as unexpected byproducts following the degradation of tris-phosphinoborate ligands. For example, the rhodium(I) complex  $[\kappa^2\text{-BP}_3^{\text{iPr}}]\text{Rh}(\text{PMe}_3)_2$  ( $[\text{BP}_3^{\text{iPr}}]$  = PhB-(CH<sub>2</sub>P<sup>i</sup>Pr<sub>2</sub>)<sub>3</sub><sup>-</sup>), undergoes reversible  $-\text{CH}_2\text{P}^{\text{i}}\text{Pr}_2$  side-arm migration at elevated temperatures to generate [PhB-(CH<sub>2</sub>P<sup>i</sup>Pr<sub>2</sub>)<sub>2</sub>]Rh(CH<sub>2</sub>P<sup>i</sup>Pr<sub>2</sub>). A related rearrangement of the  $[\text{BP}_3^{\text{iPr}}]$  ligand is observed in reactions of Na(THF)<sub>6</sub>{ $[\text{BP}_3^{\text{iPr}}]$ -CoI} with 1.5 equivs of RSiH<sub>3</sub> (R = H, Ph), in which 0.5 equiv of the respective silicide complexes  $[\text{PhB}(\text{CH}_2\text{P}^{\text{i}}\text{Pr}_2)_2]$ -(RSiH<sub>2</sub>)(H)<sub>2</sub>Co=Si=Co(H)<sub>2</sub>[BP<sub>3</sub><sup>iPr</sup>] are generated (Figure 1b). In these cases, the  $-\text{CH}_2\text{P}^{\text{i}}\text{Pr}_2$  side-arm is expelled via coupling with 0.5 equiv of RSiH<sub>3</sub> to produce  $[\text{Pr}_2\text{PCH}_2\text{SiH}_2\text{R}]$ ,

suggesting that the formation of the [PhB(CH<sub>2</sub>P<sup>i</sup>Pr<sub>2</sub>)<sub>2</sub>] ligand is mechanistically important in generating the silicide product.

For bis-phosphine borane ligands of the type [PhB-(CH<sub>2</sub>PR<sub>2</sub>)<sub>2</sub>], the P- and B-sites are in close proximity as they are linked by C<sub>1</sub> fragments. These ligands therefore offer greater rigidity than the more commonly employed examples incorporating C<sub>2</sub> linkers (frequently o-phenylene) which enable close M-B contacts. Si, 6,18,19 However, the more structurally rigid frameworks might enforce separation of an electron-rich metal center from a nearby electrophilic boron to give a situation analogous to that of "frustrated" Lewis pairs (FLPs). <sup>20,21</sup> In addition, isolation of the M- and B-centers may allow for these two sites to be independently modified (e.g., by selective coordination of a Lewis base to M or B), and should enable study of the influence of a remote electrophile on a transition metal center.

An interesting ligand in this context is  $PhB(CH_2P^tBu_2)_2$  ([BP2<sup>tBu</sup>]), which should provide significant steric demand and rigidity when coordinated to a metal center. This molecule has previously been utilized in accessing an unsymmetrical borate ligand, [PhB(CH2P^tBu2)2(pyrazolyl)]<sup>-</sup>, which functions as a  $P_1P_1N_1$ -donor ligand when coordinated to a metal center. Light when the coordinated to a metal center.

Received: July 26, 2022 Published: September 15, 2022





#### a) M-B cooperativity in substrate bond-activation:9

b) Borate to borane ligand decomposition: 17

c) Investigation of a structurally rigid borane ligand:

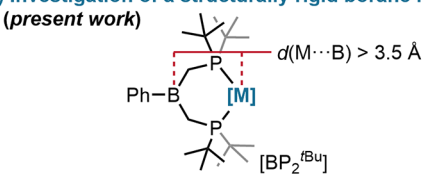


**Figure 1.** (a) Role of phosphine-borane ligands possessing close M—B contacts in substrate bond activation. (b) Spontaneous formation of a phosphine-borane ligand via borate ligand decomposition. (c) Structure of the structurally rigid phosphine-borane ligand investigated in this work.

bis-phosphino borane has not been separately examined. This work describes the synthesis, characterization, and chemical transformations of Co, Ni, and Cu complexes of the  $[BP_2^{\ fBu}]$  ligand.

## ■ RESULTS AND DISCUSSION

**Coordination Chemistry of** [BP2<sup>tBu</sup>]. The [BP2<sup>tBu</sup>] proligand was prepared via salt-metathesis of two equivs of  ${}^tBu_2PCH_2Li$  and one equiv of PhBCl2, as described by Thomas and Peters. Colorless block crystals of this compound were obtained by cooling a saturated pentane solution to  $-35\,^{\circ}C$  for 12 h. The solid-state molecular structure reveals monomeric units of [BP2<sup>tBu</sup>] with trigonal planar coordination about the boron atom [ $\Sigma_{\angle} = 359.9(3)^{\circ}$ ; see Supporting Information, Figure S1]. Furthermore, there are no apparent intermolecular interactions between P and B atoms of neighboring molecules, nor are there any intramolecular P···B interactions [ $d(P-B)_{ave} = 2.887(4)\,$ Å].

The addition of solid  $[BP_2^{tBu}]$  to THF suspensions of  $CoCl_2$ , NiCl<sub>2</sub>(1,2-dimethoxyethane), or CuCl results in rapid color changes to blue, purple, or yellow, respectively. The products of these reactions,  $[BP_2^{tBu}]CoCl_2$  ( $\mathbf{1}_{Co}$ ),  $[BP_2^{tBu}]NiCl_2$  ( $\mathbf{1}_{Ni}$ ), and [BP2 tBu] CuCl (2Cu) were obtained as bright blue, mauve, and yellow crystalline solids, respectively, after workup (Scheme 1). Complexes  $1_{Co}$  and  $1_{Ni}$  are paramagnetic with solution magnetic moments of 4.5  $\mu_{\rm B}$  and 3.0  $\mu_{\rm B}$  (Evans method), respectively; these values are consistent with S = 3/2 $(Co^{II})$  and S = 1  $(Ni^{II})$  centers in tetrahedral ligand fields. Interestingly, the  $^1H$  NMR spectra of  $\mathbf{1}_{Co}$  and  $\mathbf{1}_{Ni}$  display only modest paramagnetic shifting of resonances for the hydrogen nuclei of the Ph ring, with discernible spin-spin ( ${}^{3}J_{HH}$ ) couplings, in addition to paramagnetically shifted, broadened resonances due to the 'Bu and CH2 groups. In contrast to complexes 1<sub>Co</sub> and 1<sub>Ni</sub>, 2<sub>Cu</sub> is diamagnetic and its <sup>1</sup>H and  $^{31}P\{^{1}H\}$  NMR spectra displays sharp resonances ( $\delta_{P}$  = 22.1 Scheme 1. Syntheses of  $[BP_2^{tBu}]MCl_2$  (M = Co,  $1_{Co}$ ; M = Ni,  $1_{Ni}$ ) and  $[BP_2^{tBu}]CuCl$  ( $2_{Cu}$ )

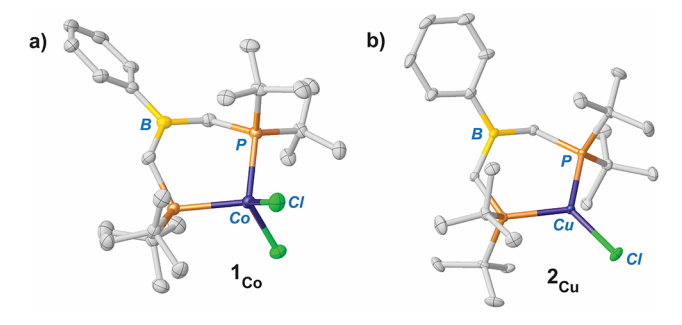


Figure 2. Solid-state molecular structures of  $\mathbf{1}_{Co}$  (a) and  $\mathbf{2}_{Cu}$  (b). Hydrogen atoms are omitted for clarity. Thermal ellipsoids are drawn at 50% probability.

ppm) that are only modestly shifted compared to those of free [BP<sub>2</sub><sup>fBu</sup>] ( $\delta_P = 38.4 \text{ ppm}^{22}$ ).

While both  ${\bf 1}_{\rm Co}$  and  ${\bf 1}_{\rm Ni}$  crystallize as long, thin needles, the crystals of  ${\bf 1}_{\rm Ni}$  were not of sufficient size to allow for X-ray structural determination. Complex  ${\bf 1}_{\rm Co}$  (Figure 2a) crystallizes with two molecules in the asymmetric unit that possess essentially identical coordination geometries about the Co centers, with the Co–P distances ranging from 2.379(2)–2.404(2) Å. As anticipated, the rigid  $[{\rm BP_2}^{\rm fBu}]$  ligand enforces a long Co···B distance [3.890(4) and 3.893(4) Å], indicating no direct Co–B interaction. The boron centers of both molecules are rigorously planar, with  $\Sigma_{\angle}=360.0(5)^{\circ}$  (averaged across both molecules). The six-membered chelate ring of the  $[{\rm BP_2}^{\rm fBu}]$  ligand is modestly puckered, with the P, Co, P and C, B, C atoms defining two planes with a torsion angle averaging  $27.5(2)^{\circ}$  for the two molecules.

The crystallographic solid-state molecular structure of  $\mathbf{2}_{\text{Cu}}$  (Figure 2b) reveals a monomeric unit possessing trigonal planar coordination at both the copper  $[\Sigma_{\angle,\text{Cu}} = 359.81(9)^{\circ}]$  and boron centers  $[\Sigma_{\angle,\text{B}} = 359.1(5)^{\circ}]$ . Unlike  $\mathbf{1}_{\text{Co}}$ , the  $[BP_2^{\text{fBu}}]$  Cu ring of  $\mathbf{2}_{\text{Cu}}$  adopts a half-chair conformation with the C, B, C fragment being puckered out of the mean plane defined by the C, P, Cu, P, C set of atoms  $[\text{fold } \angle = 50.6(4)^{\circ}]$ . The Cu··· B separation of 3.639(5) Å is smaller than that of  $\mathbf{1}_{\text{Co}}$ , likely resulting from the differing conformations of the six-membered  $[BP_2^{\text{fBu}}]M$  chelate rings.

The reduction of  $\mathbf{1}_{Ni}$  was examined as a possible route to a nickel(I) complex. Nickel(I) species remain relatively uncommon, though their unique structural and magnetic properties have attracted considerable attention. The addition of KC<sub>8</sub> to  $\mathbf{1}_{Ni}$  in toluene solution resulted in a color change from clear purple to orange over 24 h and the product,  $[BP_2^{Bu}]NiCl\ (\mathbf{2}_{Ni})$ , was isolated as an analytically pure solid following a workup (eq 1). Crystals of  $\mathbf{2}_{Ni}$  were grown by

maintaining a saturated THF solution layered with  $(Me_3Si)_2O$  at -35 °C for 18 h.

The solid-state structure of  $\mathbf{2}_{\text{Ni}}$  (Figure 3a) resembles that of  $\mathbf{2}_{\text{Cu}}$ , with a trigonal planar coordination geometry at the Ni and B centers. The Ni···B distance of 3.733(4) Å is in between the analogous metrical parameters of  $\mathbf{1}_{\text{Co}}$  and  $\mathbf{2}_{\text{Cu}}$ . The <sup>1</sup>H NMR spectrum of  $\mathbf{2}_{\text{Ni}}$  is dominated by broad, featureless resonances, and an Evans method measurement reveals a solution magnetic moment of 1.9  $\mu_{\text{B}}$ , consistent with an S=1/2 spin state. Thus,  $\mathbf{2}_{\text{Ni}}$  likely retains a monomeric structure in solution. Dimeric species with  $\mathrm{Ni_2}^{\mathrm{I}}(\mu\text{-Cl})_2$  cores often exhibit spin-pairing because of antiferromagnetic superexchange through the bridging chloride ligands, or potentially via direct Ni–Ni interactions.

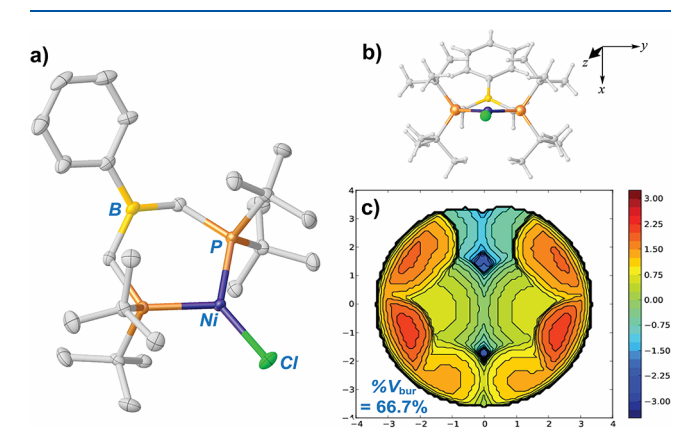


**Figure 3.** (a) Solid-state molecular structure of  $\mathbf{2}_{Ni}$ . Hydrogen atoms are omitted for clarity. Thermal ellipsoids are drawn at 50% probability. (b) View of  $\mathbf{2}_{Ni}$  along the Cl–Ni axis and coordinate system orientation. (c) Steric map of  $[BP_2^{\ fBu}]$  in  $\mathbf{2}_{Ni}$ , viewed along the Cl–Ni axis.

The monomeric structure of  $\mathbf{2_{Ni}}$  reflects the larger size of  $[\mathrm{BP_2}^{\mathrm{fBu}}]$  relative to other ligands commonly encountered in  $\mathrm{Ni^I}$  species, such as dtbpe  $[\mathrm{dtbpe} = 1,2\text{-}bis\text{-}(\mathrm{di\text{-}}tert\text{-}butylphosphino})$  ethane] or  $\mathrm{IPr}$   $[\mathrm{IPr} = 1,3\text{-}bis\text{-}(2,6\text{-}\mathrm{di\text{-}}isopropylphenyl})$  imidazole-2-ylidene], both of which support  $\mathrm{Ni_2^I}(\mu\text{-}\mathrm{Cl})_2$ -type dimers, namely,  $[(\mathrm{dtbpe})\mathrm{NiCl}]_2^{26}$  and  $[(\mathrm{IPr})\mathrm{-}\mathrm{NiCl}]_2^{27}$ . The buried volume  $(\%V_{\mathrm{bur}})$  provides a useful quantitative measure of the bulk of these ligands,  $^{30,31}$  with  $[\mathrm{BP_2}^{\mathrm{fBu}}]$   $(\%V_{\mathrm{bur}} = 66.7\%;$  Figure 3c) $^{32}$  encapsulating the metal center to a significantly greater extent than dtbpe  $(\%V_{\mathrm{bur}} = 58.4\%)^{33}$  or  $[\mathrm{IPr}$   $(\%V_{\mathrm{bur}} = 40.8\%)^{34}$ . As anticipated, the  $[\mathrm{BP_2^{\mathrm{fBu}}}]$  ligand has steric properties very similar to those of dtbpp  $[\mathrm{dtbpp} = 1,3\text{-}bis\text{-}(\mathrm{di\text{-}}tert\text{-}butylphosphino})$  propane]  $(\%V_{\mathrm{bur}} = 62.8\%)^{35}$ 

The Ni–Cl bond length of 2.163(1) Å in  $2_{Ni}$  is shorter than the analogous Cu–Cl distance of 2.213(1) Å in  $2_{Cu}$  despite the small ionic radius of the copper atom.<sup>36</sup> A qualitative energy-level molecular orbital (MO) diagram of  $[L_2]M^ICl$  complexes under  $C_{2v}$  symmetry (Figure 4) indicates that this elongation

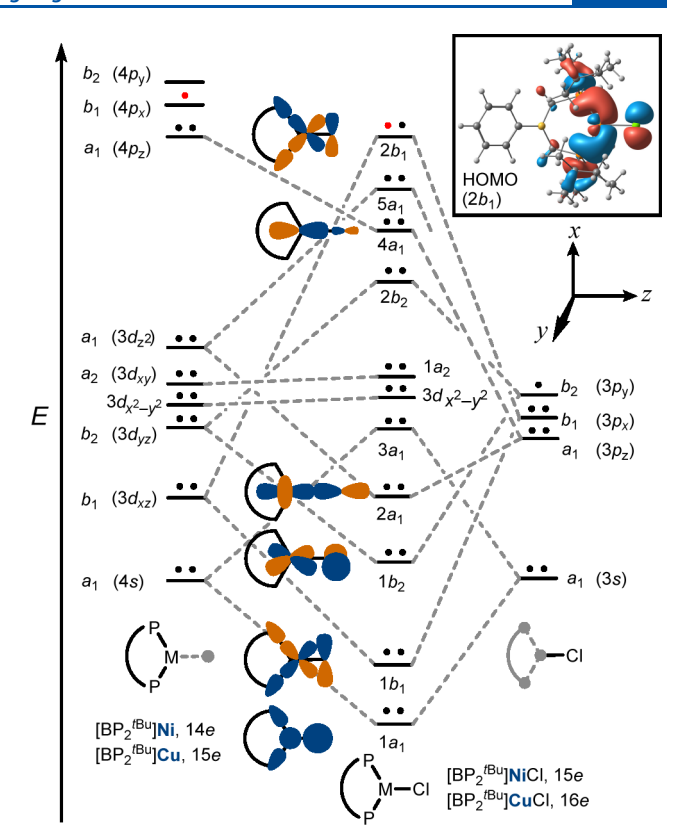


Figure 4. Qualitative MO energy-level diagram of  $[BP_2^{fBu}]$ MCl. Dots  $(\cdot)$  represent electrons; the red dot is an additional electron from Cu. Atomic orbital labels on the left-hand side (in brackets) denote transition-metal orbital parentage for  $[BP_2^{fBu}]$ M-fragment orbitals. Inset: rendering of HOMO from DFT calculations (isolevel 0.03) of  $\mathbf{2}_{Cu}$  at the  $\omega B97X\text{-}D3$  level of theory.

results from additional filling of an antibonding  $\pi^*(M-Cl)$  orbital  $(2b_1)$  in 16-electron  $\mathbf{2}_{Cu}$  compared to 15-electron  $\mathbf{2}_{Ni}$ . The additional electron in  $\mathbf{2}_{Cu}$  is represented by a red-colored dot in Figure 4. Further theoretical confirmation of this hypothesis was provided by density functional theory (DFT) computations at the  $\omega$ B97X-D3 level of theory for  $\mathbf{2}_{Cu}$ . Consistent with the qualitative MO diagram shown in Figure 4, the calculated highest-occupied MO (HOMO) is of  $\pi$ -symmetry and is dominated by Cu–Cl antibonding character (Figure 4, inset).

Cyclic voltammetric studies of  $\mathbf{2}_{Ni}$  in 1,2-difluorobenzene solution (1 mM  $\mathbf{2}_{Ni}$ , 0.1 M [ ${}^{n}$ Bu<sub>4</sub>N][PF<sub>6</sub>] electrolyte) identified a quasi-reversible wave corresponding to the Ni<sup>1</sup>/Ni<sup>II</sup> couple at -0.321 V, suggesting that the chemical oxidation of  $\mathbf{2}_{Ni}$  to regenerate  $\mathbf{1}_{Ni}$  should be possible. Indeed, the treatment of a toluene solution of  $\mathbf{2}_{Ni}$  with one equiv of trityl chloride resulted in a rapid color change from clear orange to purple, indicating the formation of dichloride complex  $\mathbf{1}_{Ni}$ . The  ${}^{1}$ H NMR spectrum of the product mixture showed that  $\mathbf{1}_{Ni}$  and Gomberg's dimer are the exclusive products of this reaction (eq 2). The products were separated by extraction of Gomberg's dimer into pentane and each was isolated in nearly quantitative yields.

Synthesis of  $[BP_2^{tBu}]M$ -Mesityl Derivatives. Attempts to affect the one electron reduction of  $\mathbf{1}_{Co}$  to generate  $[BP_2^{tBu}]$ CoCl were frustrated by apparent disproportionation pathways. Treatment of toluene or THF solutions of  $\mathbf{1}_{Co}$  with  $KC_8$ , NaHg, or zinc dust generated no tractable products, and

Ph-B Ni—CI 
$$\frac{1 \text{ equiv. Ph}_3\text{CCI}}{\text{Toluene}}$$
 Ph-B Ni—CI  $\frac{1 \text{ equiv. Ph}_3\text{CCI}}{\text{Toluene}}$  Ph-B Ni—CI  $\frac{1 \text{ equiv. Ph}_3\text{CCI}}{\text{Toluene}}$  Ph-B Ni—CI  $\frac{1 \text{ equiv. Ph}_3\text{CCI}}{\text{Toluene}}$  94%

only trace quantities of  $\mathbf{1}_{Co}$  were recovered from the reaction mixtures in addition to a black powder (presumably  $Co^0$ ) that was attracted to the poles of the magnetic stir bar. It seemed that a kinetically stable  $[BP_2^{\ fBu}]Co^I-X$  species might be isolable if disproportionation pathways were inhibited by a sufficiently bulky X group (X = alkyl, aryl).

Treatment of  $\mathbf{1}_{Co}$  with one equiv of  $Mes_2Mg(THF)_2$  in THF solution at -35 °C led to the formation of a dark green complex that was isolated as a crystalline solid following filtration and crystallization from toluene (Scheme 2). The  $^1H$ 

Scheme 2. Synthesis of  $[BP_2^{tBu}]M(Mes)$  Complexes  $(M = Co, 3_{Co}; M = Ni, 3_{Ni}; M = Cu, 3_{Cu})$ 

NMR spectrum and Evans method magnetic moment  $(3.7 \, \mu_{\rm B})$  is consistent with its formulation as  $[{\rm BP_2}^{\rm (fbu)}]{\rm Co}({\rm Mes})$  ( $3_{\rm Co}$ ), and this was confirmed by single-crystal X-ray diffraction studies (Figure 5a). Complex  $3_{\rm Co}$  is stable in benzene- $d_6$  solution for at least 5 days and can be stored indefinitely as a solid at -35 °C under an inert atmosphere. In this reaction,  ${\rm Mes_2Mg}({\rm THF})_2$  serves both to install Mes upon cobalt, and to reduce the metal center. Consistently, the  $^1{\rm H}$  NMR spectrum of the crude reaction mixture in THF solution indicates that upon reduction, an equiv of Mes· is converted into bimesitylene [82% vs  ${\rm Mes_2Mg}({\rm THF})_2$ ] and mesitylene [16% vs  ${\rm Mes_2Mg}({\rm THF})_2$ ], as determined by integration against an internal standard of  $({\rm Me_3Si})_2{\rm O}$ .

The congeneric Ni and Cu  $[BP_2^{tBu}]M(Mes)$  complexes  $(3_{Ni}, 3_{Cu})$  respectively) were readily generated by the treatment of monohalides  $2_{Ni}$  and  $2_{Cu}$  with 0.5 equiv  $Mes_2Mg(THF)_2$ . Complexes  $3_{Ni}$  and  $3_{Cu}$  were isolated as dark orange- and orange-colored crystalline solids, respectively (Scheme 2). Complex  $3_{Ni}$  is paramagnetic, as evidenced by the solution-state Evans method magnetic moment of 1.7  $\mu_B$ . Complex  $5_{Cu}$  unlike its cobalt and nickel congeners, is diamagnetic and exhibits sharp, resolved resonances in its  $^1H$ ,  $^{31}P\{^1H\}$ , and

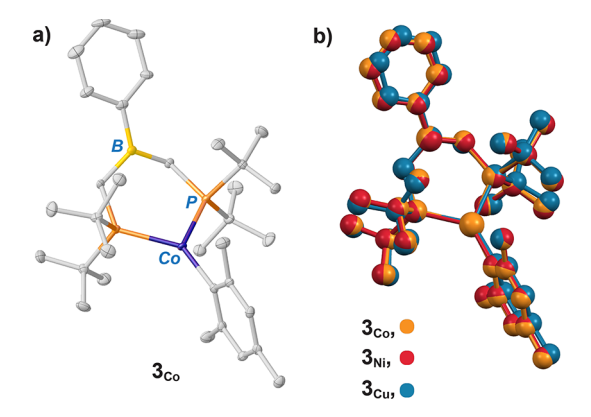


**Figure 5.** (a) Solid-state molecular structure of  $3_{Co}$ . Hydrogen atoms are omitted for clarity. Thermal ellipsoids are drawn at 50% probability. (b) Overlay of solid-state molecular structures of  $3_{Co}$ ,  $3_{Ni}$ , and  $3_{Cu}$ .

<sup>13</sup>C{<sup>1</sup>H} NMR spectra, with chemical shifts that are not influenced by pseudocontact shifts ( $\delta_P = 28.9 \text{ ppm}$ ).

Complexes  $3_{Co}$ ,  $3_{Ni}$ , and  $3_{Cu}$  crystallize in triclinic space group  $P\overline{1}$  and are essentially isostructural in the solid-state (Figure 5b). All three crystal structures exhibit twinning, suggesting that this is an inherent solid-state feature of  $[BP_2^{fBu}]M(Mes)$  molecules. In each molecule, the plane defined by the Mes ring is oriented perpendicular to the P, M, P plane.

The synthetic routes to complexes  $3_{Co}$ ,  $3_{Ni}$ , and  $3_{Cu}$  illustrate that the borane functionalities of the corresponding starting materials are resistant to nucleophilic attack by Mes<sub>2</sub>Mg-(THF)<sub>2</sub>. This feature is likely a function of the steric constraints imposed by Mes substituents, whose bulk precludes the formation of four-coordinate boron centers in this system. This is consistent with the observation that the attempted preparation of benzyl complexes of the form [BP<sub>2</sub><sup>fBu</sup>]M-(CH<sub>2</sub>Ph) (M = Co, Ni, Cu) were unsuccessful when  $1_{Co}$ ,  $2_{Ni}$ , and  $2_{Cu}$  were treated with the corresponding quantities of Mg(CH<sub>2</sub>Ph)<sub>2</sub>(THF)<sub>2</sub>, resulting instead in the formation of intractable mixtures of products in THF solution.

Lewis Base Coordination to the  $[BP_2^{\ tBu}]$  Ligand of  $2_{Ni}$ . In addition to chemical transformations occurring at the transition-metal center, the boron centers represent a second potential reaction site in  $[BP_2^{\ tBu}]$ -ligated complexes; thus, a straightforward transformation involves treatment of these complexes with a Lewis base. This type of functionalization may serve to alter the electronic properties of the complex in a remote fashion.

Addition of one equiv of 4-dimethylaminopyridine (DMAP) to  $2_{\rm Ni}$  in toluene solution resulted in rapid bleaching of the orange color, and deposition of an off-white solid after several minutes. The solid material, which is soluble in THF and 1,2-difluorobenzene, was crystallized from concentrated THF solution at -35 °C. Single-crystal X-ray diffraction analysis

of the nearly colorless blocks confirms the identity of the product to be the adduct  $[PhB(DMAP)(CH_2P^tBu_2)_2]NiCl$  (4; Figure 6).

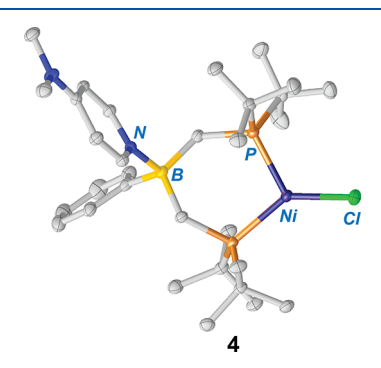


Figure 6. Solid-state molecular structure of 4. Hydrogen atoms are omitted for clarity. Thermal ellipsoids are drawn at 50% probability.

The solid-state molecular structure of 4 possesses a trigonal planar nickel center, while the boron atom is tetrahedrally coordinated with  $\tau_4$  = 0.93. The Ni–Cl bond in 4 [d(Ni–Cl) = 2.1786(6) Å] is slightly elongated (by ~0.02 Å) relative to that in  $2_{\rm Ni}$ . This minor structural change may be the result of the somewhat greater steric demands of [PhB(DMAP)-(CH<sub>2</sub>PfBu<sub>2</sub>)<sub>2</sub>] relative to the parent [BP<sub>2</sub>fBu] ligand. Another possibility is that the presumably highly electron releasing ligand sphere in 4 generates a more electron-rich nickel center that repels the chloride ligand.

To examine whether the DMAP-ligated boron center of 4 could be "deprotected", 4 was treated with one equiv of a Lewis acid,  $B(C_6F_5)_3$ . Analysis of the reaction mixture by  $^1H$  NMR spectroscopy in the presence of an internal standard  $[(Me_3Si)_2O]$  indicated that  $\mathbf{2}_{Ni}$  and DMAP- $B(C_6F_5)_3$  were formed in high yields (eq 4) as the sole products of the reaction.

The UV-visible spectra of  $\mathbf{2}_{Ni}$  and  $\mathbf{4}$  in THF solution (Figure 7) show significant differences that can be attributed to the coordination of DMAP. Notably, two major absorption features exhibited by  $\mathbf{2}_{Ni}$  at 347 nm ( $\varepsilon = 2769~\text{M}^{-1}~\text{cm}^{-1}$ ) and 328 nm ( $\varepsilon = 2956~\text{M}^{-1}~\text{cm}^{-1}$ ) are absent in the spectrum for 4, consistent with the observed colors of these complexes. On this basis, the transitions at 347 and 328 nm observed in the electronic spectrum of  $\mathbf{2}_{Ni}$  are assigned to B  $\leftarrow$  Ni charge transfer, a process which is quenched by coordinative and electronic saturation of the boron center of 4.

### CONCLUSIONS

Complexes bearing the  $[BP_2^{\ fBu}]$  ligand have been established for mono- and di-valent late 3d transition-metals. These studies illustrate that the  $[BP_2^{\ fBu}]$  ligand facilitates access to reduced organometallic species (namely,  $3_{Co}$  and  $3_{Ni}$ ) without the degradation of the borane functionality, provided that an appropriate reductant is used. The mesityl derivatives are

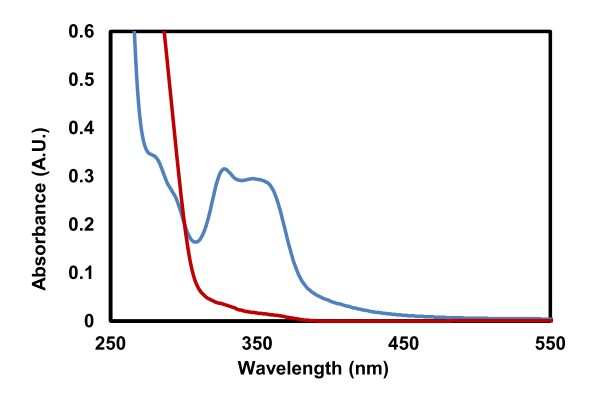


Figure 7. UV–visible spectra of  $\mathbf{2}_{Ni}$  (blue trace) and 4 (red trace) recorded in THF solution.

potentially useful starting materials for accessing metal-element bonds via addition—elimination reactions with main-group element hydrides to eliminate mesitylene. The boron center of the  $[BP_2^{\ /Bu}]$  ligand can be further modified by the coordination of a Lewis base, resulting in changes to the spectroscopic properties of the complex. This feature presents a method for tuning molecular properties by the modification of the metals' secondary coordination sphere.

#### ASSOCIATED CONTENT

### Supporting Information

The Supporting Information is available free of charge at https://pubs.acs.org/doi/10.1021/acs.organomet.2c00378.

Atomic coordinates for  $2_{Cu}$  (XYZ)

Detailed descriptions of syntheses, crystallography, computations, UV-visible spectroscopy, electrochemistry, and NMR spectra (PDF)

## **Accession Codes**

CCDC 2175406–2175413 contain the supplementary crystallographic data for this paper. These data can be obtained free of charge via <a href="www.ccdc.cam.ac.uk/data\_request/cif">www.ccdc.cam.ac.uk/data\_request/cif</a>, or by emailing <a href="data\_request@ccdc.cam.ac.uk">data\_request/cif</a>, or by contacting The Cambridge Crystallographic Data Centre, 12 Union Road, Cambridge CB2 1EZ, UK; fax: +44 1223 336033.

#### AUTHOR INFORMATION

#### **Corresponding Author**

T. Don Tilley — Department of Chemistry, University of California, Berkeley, California 94720, United States; orcid.org/0000-0002-6671-9099; Email: tdtilley@berkeley.edu

#### **Authors**

Rex C. Handford – Department of Chemistry, University of California, Berkeley, California 94720, United States;
orcid.org/0000-0002-3693-1697

Lingfei Zhong — Department of Chemistry, University of California, Berkeley, California 94720, United States;
orcid.org/0000-0001-8467-1749

Complete contact information is available at: https://pubs.acs.org/10.1021/acs.organomet.2c00378

#### Notes

The authors declare no competing financial interest.

#### ACKNOWLEDGMENTS

This work was funded by the National Science Foundation under grant no. CHE-1954808. R.C.H. thanks the NSERC of Canada for a PGS-D fellowship. This research used the resources of the Advanced Light Source, which is a DOE Office of Science User Facility under contract no. DE-AC02-05CH11231. We thank Dr. Simon J. Teat for his assistance with X-ray diffraction experiments. Computations were performed using the Tiger cluster at the Molecular Graphics and Computation Facility (MGCF) of the University of California, Berkeley, which is supported by the National Institutes of Health under grant no. NIH S10OD023532, and we thank Dr. Kathleen Durkin and Dr. Dave Small for their advice and expertise on computations. NMR spectra were recorded at the College of Chemistry NMR facility, at the University of California, Berkeley which is supported in part by the National Institutes of Health under grant no. S10OD024998; we thank Dr. Hasan Celik and Dr. Alicia Lund for advice and assistance with NMR spectroscopy. Dr. Amélie Nicolay and T. Alex Wheeler are gratefully acknowledged for their assistance and advice with cyclic voltammetry.

### REFERENCES

- (1) Parkin, G. A Simple Description of the Bonding in Transition-Metal Borane Complexes. *Organometallics* **2006**, 25, 4744–4747.
- (2) Bouhadir, G.; Bourissou, D. Complexes of Ambiphilic Ligands: Reactivity and Catalytic Applications. *Chem. Soc. Rev.* **2016**, *45*, 1065–1079.
- (3) Bouhadir, G.; Bourissou, D. Ambiphilic Ligands: Unusual Coordination and Reactivity Arising from Lewis Acid Moieties. In Ligand Design in Metal Chemistry; Stradiotto, M., Lundgren, R. J., Eds.; John Wiley & Sons, Ltd: Chichester, U.K., 2016; pp 237–269.
- (4) Braunschweig, H.; Dewhurst, R. D. Transition Metals as Lewis Bases: "Z-Type" Boron Ligands and Metal-to-Boron Dative Bonding. *Dalton Trans.* **2011**, *40*, 549–558.
- (5) Bontemps, S.; Sircoglou, M.; Bouhadir, G.; Puschmann, H.; Howard, J. A. K.; Dyer, P. W.; Miqueu, K.; Bourissou, D. Ambiphilic Diphosphine–Borane Ligands: Metal → Borane Interactions within Isoelectronic Complexes of Rhodium, Platinum and Palladium. *Chem. Eur J.* **2008**, *14*, 731–740.
- (6) Bontemps, S.; Bouhadir, G.; Miqueu, K.; Bourissou, D. On the Versatile and Unusual Coordination Behavior of Ambiphilic Ligands o-R<sub>2</sub>P(Ph)BR'<sub>2</sub>. J. Am. Chem. Soc. **2006**, 128, 12056–12057.
- (7) Sircoglou, M.; Bontemps, S.; Mercy, M.; Saffon, N.; Takahashi, M.; Bouhadir, G.; Maron, L.; Bourissou, D. Transition-Metal Complexes Featuring Z-Type Ligands: Agreement or Discrepancy between Geometry and d<sup>n</sup> Configuration? *Angew. Chem., Int. Ed.* **2007**, *46*, 8583–8586.
- (8) Moret, M.-E.; Zhang, L.; Peters, J. C. A Polar Copper–Boron One-Electron  $\sigma$ -Bond. *J. Am. Chem. Soc.* **2013**, *135*, 3792–3795.
- (9) Nesbit, M. A.; Suess, D. L. M.; Peters, J. C. E-H Bond Activations and Hydrosilylation Catalysis with Iron and Cobalt Metalloboranes. *Organometallics* **2015**, *34*, 4741–4752.
- (10) MacMillan, S. N.; Hill Harman, W.; Peters, J. C. Facile Si–H Bond Activation and Hydrosilylation Catalysis Mediated by a Nickel–Borane Complex. *Chem. Sci.* **2014**, *5*, 590–597.
- (11) Harman, W. H.; Peters, J. C. Reversible H<sub>2</sub> Addition across a Nickel–Borane Unit as a Promising Strategy for Catalysis. *J. Am. Chem. Soc.* **2012**, *134*, 5080–5082.
- (12) Harman, W. H.; Lin, T.-P.; Peters, J. C. A  $d^{10}$  Ni- $(H_2)$  Adduct as an Intermediate in H–H Oxidative Addition across a Ni–B Bond. *Angew. Chem., Int. Ed.* **2014**, *53*, 1081–1086.
- (13) Kameo, H.; Yamamoto, J.; Asada, A.; Nakazawa, H.; Matsuzaka, H.; Bourissou, D. Palladium—Borane Cooperation: Evidence for an Anionic Pathway and Its Application to Catalytic Hydro-/Deutero-dechlorination. *Angew. Chem., Int. Ed.* **2019**, *58*, 18783—18787.

- (14) Boudjelel, M.; Sadek, O.; Mallet-Ladeira, S.; García-Rodeja, Y.; Sosa Carrizo, E. D.; Miqueu, K.; Bouhadir, G.; Bourissou, D. Phosphine—Borane Ligands Induce Chemoselective Activation and Catalytic Coupling of Acyl Chlorides at Palladium. *ACS Catal.* **2021**, *11*, 3822—3829.
- (15) Seidel, F. W.; Nozaki, K. A Ni $^{0}$   $\sigma$ -Borane Complex Bearing a Rigid Bidentate Borane/Phosphine Ligand: Boryl Complex Formation by Oxidative Dehydrochloroborylation and Catalytic Activity for Ethylene Polymerization. *Angew. Chem., Int. Ed.* **2022**, *61*, No. e202111691.
- (16) Turculet, L.; Feldman, J. D.; Tilley, T. D. Coordination Chemistry and Reactivity of New Zwitterionic Rhodium and Iridium Complexes Featuring the Tripodal Phosphine Ligand [PhB-(CH<sub>2</sub>PiPr<sub>2</sub>)<sub>3</sub>]<sup>-</sup> . Activation of H–H, Si–H, and Ligand B–C Bonds. *Organometallics* **2004**, 23, 2488–2502.
- (17) Handford, R. C.; Smith, P. W.; Tilley, T. D. Activations of All Bonds to Silicon (Si-H, Si-C) in a Silane with Extrusion of [CoSiCo] Silicide Cores. *J. Am. Chem. Soc.* **2019**, *141*, 8769–8772.
- (18) Shih, W. C.; Ozerov, O. V. Selective Ortho C-H Activation of Pyridines Directed by Lewis Acidic Boron of PBP Pincer Iridium Complexes. *J. Am. Chem. Soc.* **2017**, *139*, 17297–17300.
- (19) Sircoglou, M.; Bontemps, S.; Bouhadir, G.; Saffon, N.; Miqueu, K.; Gu, W.; Mercy, M.; Chen, C.-H.; Foxman, B. M.; Maron, L.; Ozerov, O. V.; Bourissou, D. Group 10 and 11 Metal Boratranes (Ni, Pd, Pt, CuCl, AgCl, AuCl, and Au<sup>+</sup>) Derived from a Triphosphine–Borane. *J. Am. Chem. Soc.* **2008**, *130*, 16729–16738.
- (20) Flynn, S. R.; Wass, D. F. Transition Metal Frustrated Lewis Pairs. ACS Catal. 2013, 3, 2574–2581.
- (21) Stephan, D. W. Frustrated Lewis Pairs: From Concept to Catalysis. Acc. Chem. Res. 2015, 48, 306-316.
- (22) Thomas, C. M.; Mankad, N. P.; Peters, J. C. Characterization of the Terminal Iron(IV) Imides {[PhBPtBu}2(Pz')]FeIV: NAd+. J. Am. Chem. Soc. 2006, 128, 4956–4957.
- (23) Bontemps, S.; Bouhadir, G.; Dyer, P. W.; Miqueu, K.; Bourissou, D. Quasi-Thermoneutral  $P \rightarrow B$  Interactions within Diand Tri-Phosphine Boranes. *Inorg. Chem.* **2007**, *46*, 5149–5151.
- (24) Lin, C. Y.; Power, P. P. Complexes of Ni(i): A "Rare" Oxidation State of Growing Importance. *Chem. Soc. Rev.* **2017**, *46*, 5347–5399.
- (25) Bismuto, A.; Finkelstein, P.; Müller, P.; Morandi, B. The Journey of Ni(I) Chemistry. *Helv. Chim. Acta* **2021**, *104*, No. e2100177.
- (26) Mindiola, D. J.; Waterman, R.; Jenkins, D. M.; Hillhouse, G. L. Synthesis of 1,2-bis(di-tert-butylphosphino)ethane (dtbpe) complexes of nickel: radical coupling and reduction reactions promoted by the nickel(I) dimer [(dtbpe)NiCl]<sub>2</sub>. Inorg. Chim. Acta. **2003**, 345, 299–308.
- (27) Dible, B. R.; Sigman, M. S.; Arif, A. M. Oxygen-Induced Ligand Dehydrogenation of a Planar Bis- $\mu$ -Chloronickel(I) Dimer Featuring an NHC Ligand. *Inorg. Chem.* **2005**, *44*, 3774–3776.
- (28) Tsui, E. Y.; Agapie, T. Carbon Dioxide Cleavage by a Ni<sub>2</sub> Complex Supported by a Binucleating Bis(N-Heterocyclic Carbene) Framework. *Polyhedron* **2014**, *84*, 103–110.
- (29) Li, J.; Zhao, J.; Ferguson, M. J.; McDonald, R.; Ma, G.; Cavell, R. G. Synthesis, structures and reactivity of bis(iminophosphorano)-methanide chelate complexes with transition metal of cobalt, nickel, palladium and iridium. *Polyhedron* **2019**, *168*, 101–112.
- (30) Falivene, L.; Credendino, R.; Poater, A.; Petta, A.; Serra, L.; Oliva, R.; Scarano, V.; Cavallo, L. SambVca 2. A Web Tool for Analyzing Catalytic Pockets with Topographic Steric Maps. *Organometallics* **2016**, *35*, 2286–2293.
- (31) Falivene, L.; Cao, Z.; Petta, A.; Serra, L.; Poater, A.; Oliva, R.; Scarano, V.; Cavallo, L. Towards the Online Computer-Aided Design of Catalytic Pockets. *Nat. Chem.* **2019**, *11*, 872–879.
- (32)  $\%V_{\rm bur}$  was calculated for the [BP<sub>2</sub><sup>tBu</sup>]Ni fragment based on the solid-state molecular structure of  $2_{\rm Ni}$  with the following parameters: sphere r=3.50 Å, H-atoms omitted, scaled bond radii.
- (33)  $%V_{\text{bur}}$  was calculated for the (dtbpe)Ni fragment found in CCDC entry RUYMIH {corresponding to [(dtbpe)NiCl]<sub>2</sub>} with the

following parameters: sphere  $r=3.50\,$  Å, H-atoms omitted, scaled bond radii.

- (34) Clavier, H.; Nolan, S. P. Percent Buried Volume for Phosphine and N-Heterocyclic Carbene Ligands: Steric Properties in Organometallic Chemistry. *Chem. Commun.* **2010**, *46*, 841–861.
- (35) % $V_{\rm bur}$  was calculated for the (dtbpp)Ni fragment found in CCDC entry RECKUH {corresponding to [(dtbpe)Ni( $C_2H_4$ )]} with the following parameters: sphere r=3.50 Å, H-atoms omitted, scaled bond radii.
- (36) Shannon, R. D. Revised Effective Ionic Radii and Systematic Studies of Interatomic Distances in Halides and Chalcogenides. *Acta Crystallogr., Sect. A: Found. Crystallogr.* **1976**, 32, 751–767.

# **□** Recommended by ACS

# Control over Selectivity in Alkene Hydrosilylation Catalyzed by Cobalt(III) Hydride Complexes

Haiquan Yang, Xiaoyan Li, et al.

DECEMBER 01, 2022 INORGANIC CHEMISTRY

READ 🗹

# Thiolate-Bridged Heterodinuclear Manganese-Cobalt Complexes with Bridging Hydride Ligands

Kriti Pathak, Sundargopal Ghosh, et al.

NOVEMBER 03, 2022 ORGANOMETALLICS

READ 🗹

# Deoxygenating Reduction of CO<sub>2</sub> by [Cp\*Al]<sub>4</sub> to Form a (Al<sub>3</sub>O<sub>2</sub>C)<sub>2</sub> Cluster Featuring Two Ketene Moieties

Bing Wang, Herbert W. Roesky, et al.

SEPTEMBER 02, 2022 INORGANIC CHEMISTRY

READ 🗹

# Photolysis, Thermolysis, and Reduction of a Uranium Azide Complex Supported by a Double-Layer N–P Ligand

Penglong Wang, Congqing Zhu, et al.

AUGUST 15, 2022 ORGANOMETALLICS

READ **C** 

Get More Suggestions >